

Effect of metal intermixing on the Schottky barriers of Mo(100)/GaAs(100) interfaces

S. P. Hepplestone and P. V. Sushko

Citation: *Journal of Applied Physics* **116**, 193703 (2014); doi: 10.1063/1.4902009

View online: <http://dx.doi.org/10.1063/1.4902009>

View Table of Contents: <http://scitation.aip.org/content/aip/journal/jap/116/19?ver=pdfcov>

Published by the [AIP Publishing](#)

Articles you may be interested in

[Depth distribution of traps in Au/n - GaAs Schottky diodes with embedded InAs quantum dots](#)

J. Appl. Phys. **97**, 064506 (2005); 10.1063/1.1863456

[Unpinned interface Fermi-level in Schottky contacts to n- GaAs capped with low-temperature-grown GaAs; experiments and modeling using defect state distributions](#)

J. Appl. Phys. **93**, 2772 (2003); 10.1063/1.1536734

[Temperature dependent barrier characteristics of CrNiCo alloy Schottky contacts on n-type molecular-beam epitaxy GaAs](#)

J. Appl. Phys. **91**, 245 (2002); 10.1063/1.1424054

[Schottky enhancement of contacts to n- GaAs via the exchange mechanism using NiAl x Ga 1-x as a metallization](#)

J. Vac. Sci. Technol. B **17**, 432 (1999); 10.1116/1.590572

[Difference of interface trap passivation in Schottky contacts formed on \(NH₄\)₂S_x-treated GaAs and In_{0.5}Ga_{0.5}P](#)

J. Appl. Phys. **81**, 2904 (1997); 10.1063/1.365555



NEW Special Topic Sections

NOW ONLINE
Lithium Niobate Properties and Applications:
Reviews of Emerging Trends

AIP | Applied Physics Reviews

Effect of metal intermixing on the Schottky barriers of Mo(100)/GaAs(100) interfaces

S. P. Hepplestone¹ and P. V. Sushko^{2,a)}

¹Department of Physics and Astronomy, University College London, Gower Street, London, WC1E 6BT, United Kingdom

²Department of Physics and Astronomy and London Centre for Nanotechnology, University College London, Gower Street, London, WC1E 6BT, United Kingdom

(Received 8 September 2014; accepted 5 November 2014; published online 18 November 2014)

The electronic and structural properties of Mo(100)/GaAs(100) interfaces and Mo diffusion into GaAs are explored using first principle calculations. Our results show that the interface undergoes substantial atomic rearrangement with respect to the bulk structures and the bilayer of the GaAs adjacent to the interface becomes conducting. We study the *n*-type Schottky barrier height's dependence on Mo interdiffusion in the GaAs, with values ranging from ~ 0.9 eV to ~ 1.39 eV. This range is caused by the diffusants acting as additional *n*-type doping at the surface and their interaction with the metal-induced gap states. © 2014 AIP Publishing LLC.

[<http://dx.doi.org/10.1063/1.4902009>]

I. INTRODUCTION

Advances in the area of miniature microelectronic devices, such as nano-scale transistors, depend on the development of technologies that can provide higher electron mobilities and, at the same time, overcome the heat dissipation barriers in electrical contacts.¹ In turn, this requires metal-semiconductor interfaces that are Ohmic, have low resistance, and compatible with the device dimensions. Unfortunately, most metal-semiconductor interfaces form the Schottky barriers. Approaches to minimizing Schottky barrier height (SBH) are, therefore, of great interest.^{2–4}

Transistors based on III-V semiconductors possess a higher channel mobility than the traditional silicon variants and are expected to form the basis of the next generation of transistors.⁵ It was recently shown⁶ that thin layers of III-V semiconductors can be integrated into the existing silicon-based architecture. However, further advances along this path are held back by the lack of a low resistance nanoscale contact between the source/drain and the III-V channel. Although Ohmic metal/III-V semiconductor interfaces have been reported,³ without a detailed characterisation of their electronic structure, the origin of the low contact resistance remains unclear.^{7,8}

Early studies of Mo films grown on (100) surface of GaAs using electrodeposition,⁹ molecular beam epitaxy (MBE),¹⁰ ion sputtering,¹¹ and atomic layer deposition (ALD)¹² suggest that the Mo/GaAs interfaces show the Schottky rectifying behavior with *n*-type SBH values in the range of 0.55–0.9 eV (according to the *I*-*V* measurements) and 0.9–1.3 eV (according to the *C*-*V* measurements) depending on the growth conditions.¹¹ Meyer *et al.* and Batev *et al.* also showed that the Mo can form compounds with the GaAs, but only if subjected to temperatures greater than 800 K and thus, limit the temperature of their depositions to less than 800 K. These various experimental results

for the SBH show two key features, first, that the spread of results indicates that subtle variations in growth conditions can change the SBH and the second is that the *C*-*V* and *I*-*V* measurement techniques present two differing values, which has been attributed to non-uniformity at the interface, due to the approximations used.¹³ More recently, it has been shown that contacts formed by Mo metal deposited *in situ* using solid-source MBE on In_xGa_{1-x}As alloys are Ohmic and show resistance as low as $0.5 \pm 0.3 \Omega \mu\text{m}^2$.³ This result has been also been reported by Kim *et al.*¹⁴ who report a record device performance with Mo Ohmic contacts with a resistance of $7 \Omega \mu\text{m}$.

Theoretical and computational modeling of interfaces is often focused on idealized structures. At the same time, it is well known that surface chemical reactions, together with high substrate temperatures and non-negligible kinetic energies of impinging species typical for film deposition techniques, result in intermixed interfaces.¹⁵ In the case of a metal film grown on a semiconductor surface, migration of metal atoms into the semiconductor can be expected.^{2,15} Microscopic descriptions of metal interdiffusion are critical to understanding these interfaces.^{13,15,16} Here, we use *ab initio* simulations based on the density functional theory (DFT) to investigate the effect of metal diffusion on our chosen example of Mo(100)/GaAs(100) interfaces.

II. COMPUTATIONAL METHOD

Mo/GaAs interfaces were modeled using the periodic heterostructures formed by a slab of *n* atomic planes of the bulk Mo metal and a slab of *m* bilayers of GaAs. The majority of the results presented below are obtained for the heterostructure with *n* = 5 and *m* = 8 (denoted as M5GA8). Both slabs are terminated with (001) surfaces. Such heterostructures contain interfaces formed by the Ga- and As-terminated surfaces of GaAs with Mo. The Mo slab was rotated and translated in the plane of the interface so as its $\langle 100 \rangle$ vector forms 11.4° angle with $\langle 110 \rangle$ vector of GaAs in order to generate commensurate low-strain Mo/GaAs interface. In

^{a)}Present address: Fundamental and Computational Sciences Directorate, Pacific Northwest National Laboratory, Richland, WA 99352, USA

addition, energy changes due to the translation of the Mo and GaAs slabs with respect to each other were found to be insignificant compared to the binding and reconstruction energies.

The calculations were carried out using the PBE exchange-correlation functional¹⁷ and the projected augmented waves method¹⁸ implemented in the Vienna *ab initio* simulation program.¹⁹ A plane-wave basis set with the 500 eV energy cutoff and $5 \times 5 \times 2$ Monkhorst-Pack k -grid were used. The total energy of each system was minimized with respect to the internal coordinates and the lattice parameters. The SBH was calculated following the standard approach, which relies on referencing the relevant energies to the local potential as described elsewhere.^{20,21} Furthermore, to provide further evidence as to the value of the SBH, we also carried out calculations using the HSE06²² hybrid functional and note that the SBH does not change with the choice of functional. While the results presented below are obtained for the M5GA8 heterostructure, similar properties are obtained for a range of heterostructures with the Mo slab thickness varying between 3 and 9 atomic planes and the GaAs slab thickness ranging from 4 to 12 bilayers.

III. RESULTS AND DISCUSSION

Fig. 1 shows the atomistic structure of the M5GA8 heterostructure both prior to and after relaxation. The Mo part of the interface is little perturbed with respect to the ideal bulk lattice. This is consistent with the high cohesive energy of the bulk Mo: 7.03 eV per atom in our calculations and 6.84 eV according to the experimental measurements.²³ In contrast, the near-interface Ga and As atomic planes undergo dramatic relaxation. (For comparison, the calculated and experimentally measured²⁴ cohesive energies of GaAs are 3.16 and 3.0 eV, respectively.)

To demonstrate the character of this relaxation better we show the arrangement of the As and Mo atoms near the As-terminated interface in Figs. 1(a) and 1(b) and the corresponding Ga-terminated interface in (c) and (d). As a result

of the energy minimization, the As atoms in the outermost plane displace into the *bcc* lattice sites continuing the tessellation of the Mo lattice. The distance across the interface between the As and Mo atoms across the interface ranges between 2.5 and 2.8 Å. This distortion results in the As-As distances being up to 0.9 Å smaller than the distance between the same atoms in the bulk GaAs. Ga ions in the second plane from the interface are also displaced and the distances between them and the nearest As atoms are increased by up to 0.2 Å when compared to the bulk GaAs. Similar behavior is observed at the Ga-interface, with the Ga-Ga atom interatomic distance is reduced by up to 0.7 Å. Such relaxation can be rationalised as the “hard” Mo film inducing the strong deformation of the near-interface region in the “soft” GaAs lattice. This suggests that the strain induced by the GaAs substrate on the Mo film is negligible. Therefore, the Mo growth mode is determined by the relative magnitudes of the bulk cohesive energy and formation energies of surfaces. Since the formation energy for Mo(100) surface is 0.21 eV/Å²,²⁵ Mo is expected to grow in a layer-by-layer mode, which is consistent with experimental data.¹¹

To calculate the formation energy of the Ga- and As-terminated interfaces with Mo, we follow the standard procedure for polar interfaces²⁶

$$E_f = E_T - n_{Mo}\mu_{Mo} - n_{GaAs}\mu_{GaAs} \pm n_{As}\mu_{As}, \quad (1)$$

where E_T is the total energy of the combined heterostructure, n_{Mo} is the number of Mo, μ_{Mo} is the chemical potential of Mo (atomic energy of Mo in its bulk state), n_{GaAs} is the number of GaAs pairs, and μ_{GaAs} is the chemical potential of GaAs (the total energy of a pair of GaAs atoms in bulk). For systems with identical terminations, n_{As} is the difference between the number of As and Ga atoms. The chemical potential of As is then calculated either from bulk As (As-rich conditions), or from $\mu_{As} = m\mu_{GaAs} - \mu_{Ga}$, where μ_{Ga} is calculated from bulk Ga and corresponds to Ga rich conditions. Hence, we considered a system consisting of 3

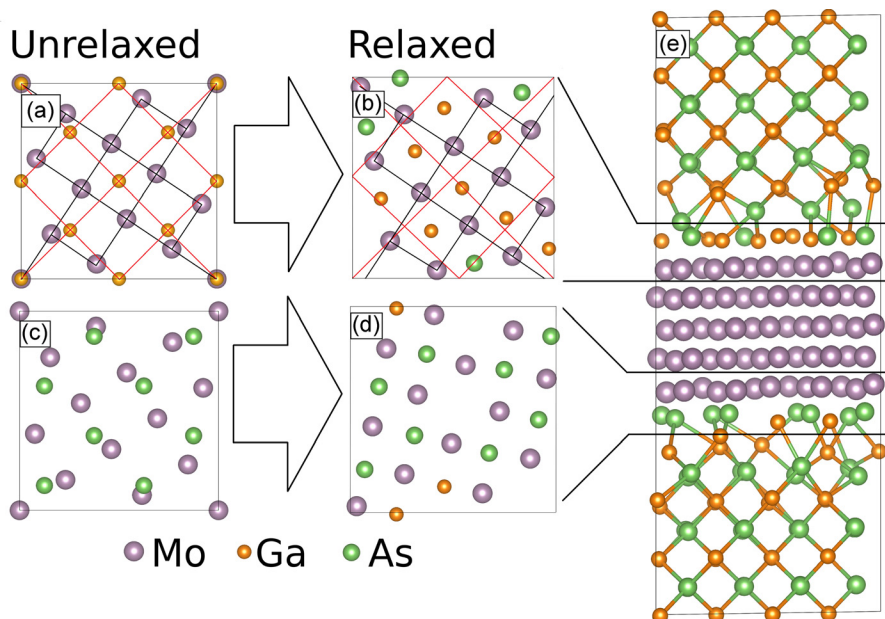


FIG. 1. The bulk and relaxed atomic structure at the As-terminated [(a) and (b)] and Ga-terminated [(c) and (d)] interface and the complete relaxed unit cell in panel (e). The Mo/As/Ga atoms are shown as purple/green/orange spheres (in the order of increasing size). In (a) and (b), we highlight the *bcc* and *fcc* lattices.

monolayers of Mo and 7 bilayers of GaAs with an additional either Ga or As layer resulting in a heterostructure, where the GaAs slab has two either As-terminated or Ga-terminated surfaces. The calculated formation energy of the Mo/As interface is $0.07 \text{ eV}/\text{\AA}^2$ in the As-rich limit and $0.09 \text{ eV}/\text{\AA}^2$ in the Ga-rich limit. The formation energy of the Mo/Ga interface is 0.10 and $0.12 \text{ eV}/\text{\AA}^2$ for the Ga- and As-rich limits, respectively. These high formation energies (compared to other GaAs interfaces²⁰) are a result of the GaAs atoms being significantly distorted from their bulk structure.

Bader analysis [see Fig. 2(a)] suggests that electron density is transferred from the near-interface Mo atomic plane to the two nearest atomic planes of GaAs. As expected, in both Ga- and As-terminated interfaces, most of the transferred charge is associated with the Ga atoms, which provide the dominant contribution to the bottom of the GaAs conduction band. Due to the higher electronegativity of As, a greater amount of charge, as calculated for the bi-layer adjacent to the interface, is transferred across the Mo-As interface ($-5.0 |e|$) than across the Mo-Ga interface ($-3.3 |e|$). As a result, the average charge on the As atoms increases from the bulk value of $-0.67 |e|$ to $-0.72 |e|$ and $-0.94 |e|$ for the Mo-Ga and Mo-As interfaces, respectively. Similarly, the Ga atoms become negative as their charge changes from the bulk value of $+0.66 |e|$ to $-0.37 |e|$ (Mo-As) and $\sim -0.1 |e|$ (Mo-Ga). As a result of the charge transfer, the electrostatic interaction between the near-interface As and Mo becomes stronger, which is reflected in the larger displacements of the As atoms towards the Mo film than the Ga. According to the theory of metal-semiconductor interfaces (see Monch²⁷ and references therein), this charge transfer results in the formation of metal-induced gap states (MIGS), which are discussed below.

The electronic density of states projected on each atomic layer (LPDOS) is shown in Fig. 2(b). The LPDOS for the atoms in the bilayers adjacent to the interfaces show non-zero density of states at the Fermi energy indicating that the near-interface region of the GaAs becomes conductive. Moreover, the LPDOS in the GaAs part of the heterostructure near the interface is similar to that of the bulk Mo part. This suggests that the closure of the GaAs band gap in this

region is induced by the Mo states extending into the GaAs (the MIGS) rather than by the Mo-induced rearrangement of the Ga and As atoms. However, a band gap appears 5.7 \AA away from the interface in the semiconductor region and it increases with increasing distance from the Mo layer and reaches its theoretical bulk value at 11.3 \AA .

To quantify the effect of the atomic rearrangement on the GaAs band gap, we calculated the LPDOS for the GaAs slab alone in the atomic configuration obtained for the Mo/GaAs heterostructure, which showed several small gaps in the LPDOS for the surface layer, whereas the LPDOS for the GaAs atoms in the heterostructure has no zero states. Hence, we can state that the atomic reconfiguration of the GaAs (compared to its ideal bulk structure) is insufficient to produce the continuous LPDOS shown in Figure 2 for the GaAs bilayers adjacent to the interface. An additional contribution to the LPDOS in the GaAs region comes from the MIG states extending into the GaAs. These MIGS can be seen in Figure 2 as the continuous non-zero LPDOS for the GaAs layers adjacent to the interface. The contribution of these states to the LPDOS decreases with increasing distance from the interface. However, importantly, they only appear in the presence of the metal. The extent of the charge transfer at the interface can be quantified using the Bader analysis of the charge density, which suggests that $\approx 6.2 |e|/\text{nm}^2$ are transferred from the Mo slab into the GaAs region. Hence, for the combined Mo/GaAs structure, we can state that the lack of a band gap in the LPDOS in the adjacent bilayers of the GaAs to the interface is due to the MIGS, not the atomic rearrangement.

To calculate the SBH, we compare two systems consisting of 5 monolayers of Mo and 6 bilayers of GaAs with an additional either Ga or As layer resulting in heterostructures, where the GaAs slab has two either As- or Ga-terminated surfaces. For the Ga-terminated interface, we calculate the *p*-type SBH to be 0.1 eV and for the As-terminated interface, we find the SBH to be 0.2 eV . Thus, given the multitude of terminations for GaAs, we expect the variation in the SBH to $0.1\text{--}0.2 \text{ eV}$ depending on the conditions the GaAs is grown in. From these values, the *n*-type SBH is implied to be $1.2\text{--}1.3 \text{ eV}$ (using a scissoring technique²¹ and the bulk band gap of GaAs (1.42 eV) at room temperature). The *n*-type SBH matches with the high end of the range of values determined using the capacitance measurements by Meyer,¹¹ who also measured a value of 1.3 eV for their SBH. However, this is one of a range of values reported¹⁰ and the result presented here clearly does not account for this range.

In the main message of this paper, we focus on the effect of the mixing of Mo into the GaAs region. We study this by adding a Mo interstitial to the M5GA8 unit cell at various sites and calculating the resulting properties such as formation energy and Schottky barrier height. These Mo interstitials act as *n*-type dopants, which change the resultant properties of the interface. The formation energy per unit cell of the Mo interstitials is defined as

$$E_f = E_{T,I} - E_H - \mu_{\text{Mo},i}, \quad (2)$$

where $E_{T,I}$ is the total energy of the heterostructure with a Mo interstitials in the GaAs region, E_H is the total energy of

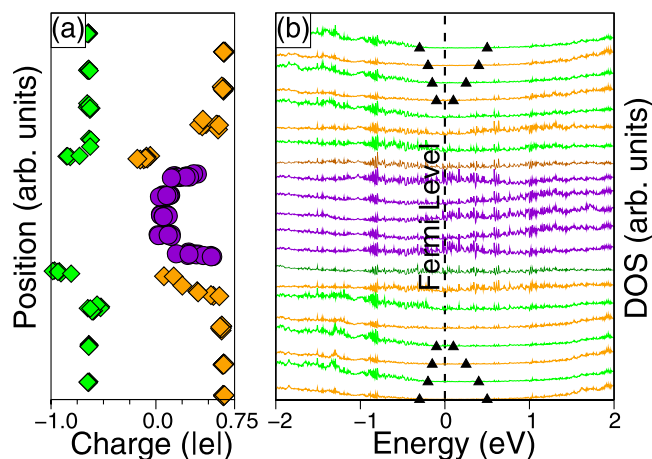


FIG. 2. (a) Bader charge analysis and (b) the layer projected density of states. The Fermi level in panel (b) corresponds to zero eV. The purple/orange/yellow/blue colours correspond to Mo/Ga/As/(Ga and As) atomic layers as shown in Fig. 1.

the heterostructure without the interstitial, and $\mu_{Mo,i}$ is the chemical potential of Mo (taken as the total energy of an isolated Mo atom). Our calculated values for the formation energies of the interstitial Mo atoms as a function of distance from the interface are shown in Fig. 3(a). The formation energy fits an exponential decline indicating that the MIGS and the resultant charge transfer are responsible for the lowering of the formation energy when compared to the bulk value of Mo interstitials in GaAs.

Our results suggest that Mo interstitials in Mo/GaAs structures can be assigned to one of the three types. (i) Mo atoms adjacent to the interface, (ii) Mo atoms located away from the interface but in the region affected by the MIG states, and (iii) Mo atoms located far from the interface. These are shown in Figure. 3.

Type I interstitials consist of an additional Mo atom adjacent (i.e., within 3 Å) to the interface. These atoms are not true interstitials, as they conform to the same *bcc* structure as the Mo slab and the distorted adjacent bilayer of GaAs similar to what is shown in Figs. 1(b) and 1(d). This positioning of the Mo interstitial is due to the very high cohesive energy of Mo, which makes it favourable for a Mo atom to occupy a site corresponding to the bulk Mo lattice. These Mo will tend to be 0.1 Å closer to As atoms than Ga atoms, but the dominating geometric consideration is the continuation of the Mo *bcc* structure. In addition, introducing these Mo atoms reduce the strain in both the Mo layer and the GaAs layer by up to 1% depending on its exact location in the GaAs plane.

Analysis of the LPDOS (see Figure 3(b)) and charge density show that Type I defects extend the reach of the MIGS in the GaAs by an additional bilayer. The figure also shows the interstitial's PDOS reflects that of the metallic Mo region, further supporting the Mo becoming a continuation of the Mo slab.

The small variation in SBH shown in Fig. 3 for Type I interstitials is due to the different numbers of Ga and As

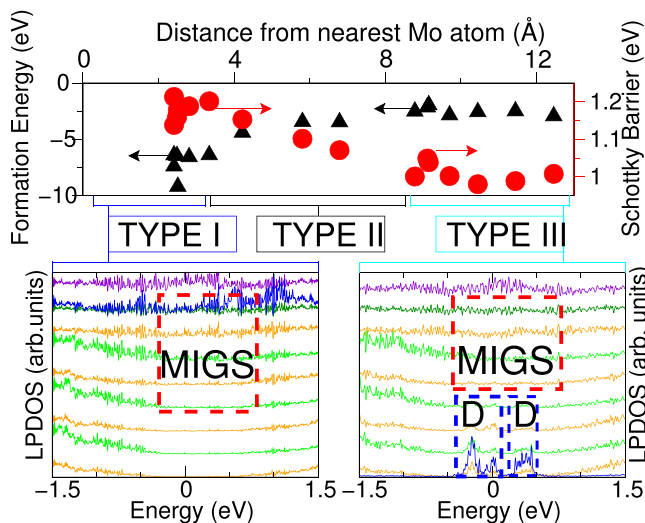


FIG. 3. (a) Calculated values for the formation energy and *n*-type Schottky barrier height as a function of position of the Mo interstitial, (b) and (c) the LPDOS of the Mo/GaAs interface, with MIGS and interstitials defect states (D) highlighted. The Mo/Ga/As atomic planes are shown in purple/orange/green with the Mo interstitial shown overlaid in blue.

atoms adjacent in the local environment of the interface. We find that, in general, this atomic scale protrusion decreases the *n*-type SBH by ≈ 0.1 eV.

By comparing the highly favorable formation energy (-14 eV per unit cell) of these interstitials with the cohesive energy of bulk Mo (7.0 eV per atom), we can infer that Mo layers grown with these intrusions into the GaAs are energetically far more likely than abrupt interfaces. Hence, these interfaces are likely to include Mo protrusions in agreement with Blank *et al.*² who discuss that much larger protrusions lead to short circuits in devices.

Type II defects are classed as Mo interstitials located between 3 and 9 Å away and are defined by two requirements: (i) the interstitial Mo atoms are not directly bound to the Mo slab and (ii) their location lies in the GaAs region in the original system (shown in Fig. 1), where the corresponding LPDOS has MIGS and no band gap.

This interstitial Mo atom occupies a site approximately at the center of the cage in the GaAs zinc-blende structure with a slight shift towards both the Mo slab and the adjacent As atoms. The resulting Mo–As and Mo–Ga distances are 2.4–2.7 Å and 2.5–2.6 Å, respectively, with very little distortion on the adjacent GaAs.

The LPDOS for these structures appears as a mix of Types I and III, with the overlap between MIGS and the Mo defect states unclear due to heavy intermixing of the two sets of states. Examining the LPDOS for these structures reveals that the opening of the band gap occurs much further (up to 16 Å from the interface) into the semiconductor depending on the location of the interstitial. Bader charge analysis also shows that these Type II Mo interstitials act as *n*-type dopants, transferring $\approx 0.8 |e|$ to the surrounding GaAs, mainly the nearest As atoms and not to the Mo slab region.

The formation energy of Type II defects is lower by up to 5 eV compared to Type III and Mo interstitials in bulk GaAs, as seen in Fig. 3. This is due to the overlap of the MIGS with the interstitial's states. Comparison of these energies with those of oxygen defects²⁸ suggests that Type II interstitials are present at interfaces, but in reduced quantities compared to Type I.

Type III interstitials are located at a distance greater than 9 Å from the interface (i.e., outside the range of MIG states induced by the Mo slab) are similar to those in the bulk GaAs. The energies of formation of such defects are between 0 and -2 eV with the small variation being due to the slight variation in the cell geometry, and slight tail off of the MIGS (due to the exponential decay). Figure 3(c) shows the change to the LPDOS when an isolated Mo interstitial atom is introduced into GaAs region of the supercell far from the interface. From the figure, we can clearly identify interstitials defect states (D-states in Fig. 3) and MIGS. The electronic states induced by an isolated Mo defect atom spread as far as three atomic planes away from the interstitial site.

For Type III, interstitials show three key features: (i) the electrons in these interstitials are localized in directional bonds between the Mo and As atoms; (ii) the metallic states in the Mo slab are unaffected by the Mo interstitials; and (iii) the Mo atom donates $0.8 |e|$ to the surrounding system, with

the majority being donated to the local GaAs and up to $0.1 |e|$ is transferred to the Mo slab.

The Mo interstitial atom is located closer to the As (2.5 \AA) than the Ga atoms (2.6 \AA) slightly distorting the local structure. This distortion is smaller than observed in Type I and Type II cases. Compared to GaAs bulk, the tetrahedral structure surrounding the interstitial is slightly distorted causing the Ga-As-Ga bond angle to increase to 115° on average and decrease the As-Ga-As bond to less than 108° .

Figure 3(a) shows the SBH for the Mo(100)/GaAs(100) system as a function of distance between the Mo slab and the Mo interstitial. The interstitials act as *n*-type dopants, which result in the Fermi level moving towards the conduction band. Type I interstitials are in effect part of the Mo slab, and as such, the SBH shift is minimal. Type II interstitials lie in the region of the MIGS, which provide additional charge to the region and effectively mask the *n*-type doping. This effect reduces the SBH slightly. Finally, Type III acts as pure *n*-type dopants, which result in an increase in the Fermi energy when compared to the ideal case and hence a decreased SBH. These results show that the discrepancy and range of results for Mo/GaAs SBH reported previously is due to the migration of Mo interstitials into the GaAs, which is dependent on growth directions. This is in clear agreement with the hypothesis of Coskun *et al.*, who suggest that intermixing and non-abrupt contacts cause the variation in experimental SBH data.¹³

IV. CONCLUSION

The electronic properties of the Mo(100)/GaAs(100) interface have been explored using *ab initio* simulations. We find due to the strong interaction at the interface that the local configuration of Ga and As atoms is considerably different from their bulk structure. We believe this to be due to the strong interaction of the Mo slab with the adjacent GaAs atoms. We have also explored the effect of Mo interstitials in the GaAs region on the properties of Mo/GaAs interfaces. The low energies of formation for these interstitials suggest mean that abrupt interfaces are very unlikely and that protrusions of the Mo into the GaAs can be expected. The low formation energy of these protrusions is due to the very high cohesive energy of the Mo atoms when compared to the GaAs. These interstitials both reduce lattice strain and also decrease the *n*-type SBH due to the additional *n*-type doping they introduce into the GaAs region. As such, the Mo interstitials change the SBH by up to 0.4 eV providing strong evidence to the cause in the range of reported results in the literature for different samples. Finally, our results show that metal/semiconductor contacts modelled as for abrupt interfaces will not produce accurate results for the electronic properties, as intermixing and doping effects will significantly change these. Hence for the further development of metal/

semiconductor contacts and their modelling, the diffusion of the metal into the semiconductor is critical to understanding the SBH and hence the resultant device properties.

ACKNOWLEDGMENTS

The authors are grateful to A. L. Shluger, S. A. Chambers, K. Kalna, and M. Aldegunde for stimulating discussions. S.P.H. was supported by the EPSRC Grant No. EP/I009973/1, P.V.S. was supported by the Royal Society. Access to the HECToR high-performance computing facility was made available via our membership of the UK's HPC Materials Chemistry Consortium, which was funded by EPSRC (EP/F067496).

- ¹M. J. Rodwell, M. Le, and B. Brar, *Proc. IEEE* **96**, 271 (2008).
- ²T. V. Blank and Y. A. Gol'dberg, *Semiconductors* **41**, 1263 (2007).
- ³U. Singiseti, M. A. Wistey, J. D. Zimmerman, B. J. Thibeault, M. J. W. Rodwell, A. C. Gossard, and S. R. Bank, *Appl. Phys. Lett.* **93**, 183502 (2008).
- ⁴A. G. Baca, F. Ren, J. C. Zolpera, R. D. Briggs, and S. J. Pearton, *Thin Solid Films* **308–309**, 599 (1997).
- ⁵J. A. del Alamo, *Nature* **479**, 317 (2011).
- ⁶H. Ko, K. Takei, R. Kapadia, S. Chuang, H. Fang, P. W. Leu, K. Ganapathi, E. Plis, H. S. Kim, S.-Y. Chen, M. Madsen, A. C. Ford, Y.-L. Chueh, S. Krishna, S. Salahuddin, and A. Javey, *Nature* **468**, 286 (2010).
- ⁷R. Dormaier and S. E. Mohney, *J. Vac. Sci. Technol.*, **B 30**, 031209 (2012).
- ⁸R. T. Tung, *Appl. Phys. Rev.* **1**, 011304 (2014).
- ⁹K. Suh, H. K. Park, and K. L. Moazed, *J. Vac. Sci. Technol.*, **B 1**, 365 (1983).
- ¹⁰J. Bloch, M. Heiblum, and Y. Komem, *Appl. Phys. Lett.* **46**, 1092 (1985).
- ¹¹F. Meyer, E. Velu, C. Pellet, C. Schwebel, and C. Dupas, *Rev. Phys. Appl.* **23**, 933 (1988).
- ¹²P. M. Batev, M. D. Ivanovitch, E. I. Kafedjiiska, and S. S. Simeonov, *Int. J. Electron.* **48**, 511 (1980).
- ¹³C. Cockun, S. Aydogan, and H. Efeoglu, *Semicond. Sci. Technol.* **19**, 242 (2004).
- ¹⁴T.-W. Kim, D.-H. Kim, and J. del Alamo, IEEE International Electron Devices Meeting (IEDM) 30.7.1 (2010).
- ¹⁵S. A. Chambers, M. H. Engelhard, V. Shutthanandan, Z. Zhu, T. C. Droubay, L. Qiao, P. V. Sushko, T. Feng, H. D. Lee, T. Gustafsson, E. Garfunkel, A. B. Shah, J.-M. Zuo, and Q. M. Ramasse, *Surf. Sci. Rep.* **65**, 317 (2010).
- ¹⁶Y.-i. Matsushita and A. Oshiyama, *Phys. Rev. Lett.* **112**, 136403 (2014).
- ¹⁷J. P. Perdew, K. Burke, and M. Ernzerhof, *Phys. Rev. Lett.* **77**, 3865 (1996).
- ¹⁸P. E. Blöchl, *Phys. Rev. B* **50**, 17953 (1994).
- ¹⁹G. Kresse and D. Joubert, *Phys. Rev. B* **59**, 1758 (1999).
- ²⁰K. T. Delaney, N. A. Spaldin, and C. G. V. de Walle, *Phys. Rev. B* **81**, 165312 (2010).
- ²¹K. T. Butler and J. H. Harding, *J. Phys.: Condens. Matter* **25**, 395003 (2013).
- ²²J. Heyd, G. E. Scuseria, and M. Ernzerhof, *J. Chem. Phys.* **118**, 8207 (2003).
- ²³M. J. Zhu, D. M. Bylander, and L. Kleinman, *Phys. Rev. B* **36**, 3182 (1987).
- ²⁴M. Causá, R. Dovesi, and C. Roetti, *Phys. Rev. B* **43**, 11937 (1991).
- ²⁵M. J. Mehl and D. A. Papaconstantopoulos, *Phys. Rev. B* **54**, 4519 (1996).
- ²⁶S. B. Zhang and J. E. Northrup, *Phys. Rev. Lett.* **67**, 2339 (1991).
- ²⁷W. Mönch, *Rep. Prog. Phys.* **53**, 221 (1990).
- ²⁸W. Orellana and A. C. Ferraz, *Phys. Rev. B* **61**, 5326 (2000).